A THESIS
on

TEMPLATE ASSISTED SYNTHESIS OF Cu-CdSe-Cu NANOWIRE HETROJUNCTIONS AND THEIR CHARACTERIZATION

Submitted in the partial fulfillment of requirement for the award of the Degree of

Master of Technology (Materials and Metallurgical Engineering)

Submitted by

RITESH PATEL

Roll No: 600802020

Under the guidance of

Dr. N.K. VERMA

Professor and Dean

School of Physics & Materials Science

Thapar University

Patiala (Punjab) - 147004

July 2010

CERTIFICATE

This is to certify that the thesis entitled **"Template Assisted Synthesis of Cu-CdSe-Cu Nanowire Hetrojunctions"** submitted By **Ritesh Patel, Roll no. 600802020** in the partial fulfillment of the requirement for the award of the degree **M. Tech** in **Materials and Metallurgical Engineering** from the School of Physics and Materials Science, Thapar University, Patiala, is a record of candidate's own work carried out by him under my supervision and guidance. The matter embodied in this report has not been submitted in part or full to any other university or institute for the award of any degree.

(Dr. N.K.Verma)

Professor & Dean, Student Affairs,

School of Physics and Materials Science

Thapar University, Patiala-147004 (Punjab)

Countersigned by:

(Dr. O.P. Pandey)

Professor & Head,
School of Physics and Materials Science,
Thapar University,
Patiala-147004 (Punjab).

(Dr. R.K.Sharma)

Dean, Academic Affairs,
Thapar University,
Patiala-147004 (Punjab)

Dated:

ACKNOWLEDGMENT

The real spirit of achieving a goal is through the way of excellence and discipline.

I would have never succeeded in completing my task without the cooperation, encouragement and help provided to me by various personalities.

With deep sense of gratitude I express my sincere thanks to my esteemed and worthy supervisor Dr. N.K. Verma, Professor, School of Physics and Material Science, for his valuable guidance in carrying out this work under his effective supervision, encouragement, enlightens and cooperation.

I shall be failing in my duties if I do not express my deep sense of gratitude towards Dr. O. P. Pandey, Professor and Head, School of Physics and Materials Science, who has been a constant source of inspiration for me throughout this work.

I wish my heartfelt thanks to research scholars Mr. Gurmeet Singh, Mr. Sanjeev Kumar, Mr. Jaspal Singh, Ms. Manveen Kaur and Shveta Kakkar for their generous help and good wishes.

I owe my sincere thanks to all the staff members of School of Physics and Materials Science for their support and encouragement.

Above all I render my gratitude to the ALMIGHTY, who bestowed self-confidence, ability and strength in me to complete this work.

(RiteshPatel)

(600802020)

ABSTRACT

The Cu-CdSe-Cu Nanowire Heterojunctions were fabricated by sequential electrodeposition of layers of Cu and the semiconductor CdSe within porous anodic aluminum oxide (AAO) template.The growth and microstructural study of nanowire Heterojunctions has been made using scanning electron microscope (SEM). The structural and phase analysis of nanowire heterojunctions has been done by X-Ray Diffraction (XRD). X-ray diffraction investigations revealed that the CdSe segment with wurzite structure and hexagonal phase, Cu with tetragonal structure has been grown. The quantitative elemental analysis of the nanowire Heterojunctions has been made by Energy Dispersive X-Ray Spectroscopy (EDAX).The collective nonlinear I–V characteristics were observed, which reveals rectifying behaviour of nanowire heterojunctions.

Content

CHAPTER 3: Experimental Details

CHAPTER 4: Results and Discussion

List of Figures

List of Tables

CHAPTER 1
Introduction

1.1 Introduction to Nanoscience and Nanotechnology

Nanotechnology is the study of the controlling of matter on an atomic or molecular scale. Nanoscience deal with structures sized between 1 to 100 nanometer, in at least one dimension and involves developing materials or devices within that size. Nanotechnology is very diverse, ranging from extensions of conventional device physics to completely new approaches based upon molecular self-assembly, from developing new materials with dimensions on the nanoscale to investigating whether we can directly control matter on the atomic scale [1, 2]. There has been much debate on the future implications of nanotechnology. Nanotechnology has the potential to create many new materials and devices with a vast range of applications, such as in medicine, electronics, biomaterials and energy production. On the other hand, nanotechnology raises many of the same issues as with any introduction of new technology, including concerns about the toxicity and environmental impact of nanomaterials and their potential effects on global economics, as well as speculation about various doomsday scenarios. These concerns have led to a debate among advocacy groups and governments on whether special regulation of nanotechnology is warranted [3]. One nanometer (nm) is one billionth, or 10^{-9}, of a meter. By comparison, typical carbon-carbon bond lengths, or the spacing between these atoms in a molecule, are in the range 0.12–0.15 nm, and a DNA double-helix has a diameter around 2 nm. On the other hand, the smallest cellular life-forms, the bacteria of the genus Mycoplasma, are around 200 nm in length. Two main approaches are used in nanotechnology. In the "bottom-up" approach, materials and devices are built from molecular components which assemble themselves chemically by principles of molecular

recognition. In the "top-down" approach, nano-objects are constructed from larger entities without atomic-level control. In the last decade, new directions of modern research have been broadly defined as “nanoscale science and technolog”. Many nanoforms of matter exist around us. One of the earliest nano-sized objects known to us is made of gold. Faraday prepared colloidal gold in 1856 and called it “Divided metals”

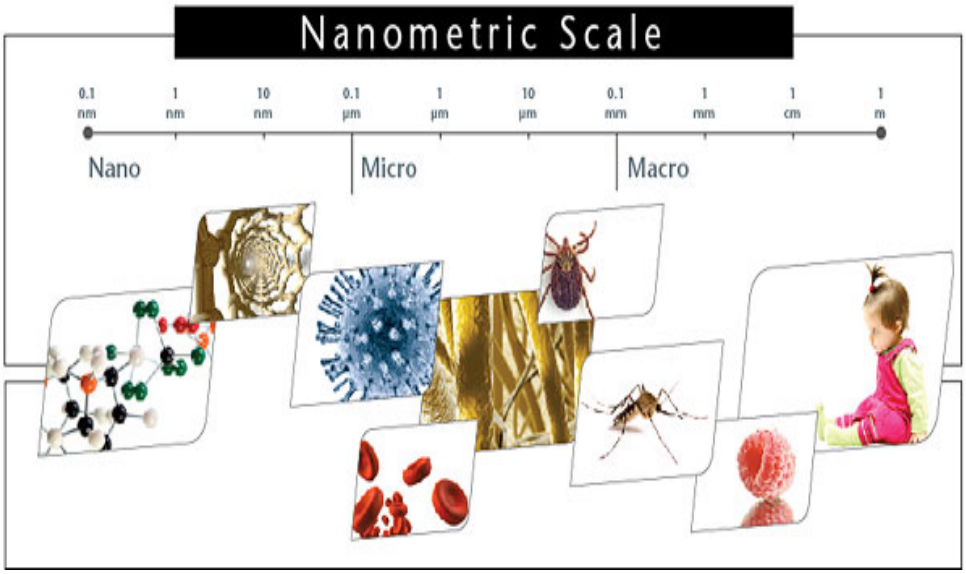

Figure 1.1: The illustrations of different scale

The first mention of some of the distinguishing concepts in nanotechnology was in "There's Plenty of Room at the Bottom", a talk given by Richard Feynman at an American Physical Society meeting Caltech on December 29, 1959. Feynman described a process by which the ability to manipulate individual atoms and molecules might be developed, using one set of precise tools to build and operate another proportionally smaller set, so on down to the needed scale. In the course of this, he noted, scaling issues would arise from the changing magnitude of various physical phenomena: gravity would become less important, surface tension and van der Waals attraction would become more important, etc. The term "nanotechnology" was defined by Tokyo Science University Professor Norio Taniguchi in a 1974 paper as follows: “Nanotechnology mainly consists of the processing, separation, consolidation, and deformation of materials by one atom or

one molecule." as shown in Figure 1.1. In the 1980s the basic idea of this definition was explored in much more depth by Dr. Eric Drexler, who promoted the technological significance of nanoscale phenomena and devices through speeches and the books "Engines of Creation: The Coming Era of Nanotechnology" and "Nanosystems: Molecular Machinery, Manufacturing, and Computation", and so the term acquired its current sense[4,5].

1.2 Introduction to Nanowires

One-dimensional nanostructures have been called by a variety of names including: whiskers, fibers or fibrils, nanowires and nanorods. In manycases, nanotubules and nanocables are also considered one-dimensional structures. Although whiskers and nanorods are in general considered to be shorter than fibers and nanowires. In addition, one-dimensional structures with diameters ranging from several nanometers to several hundred microns were referred to as whiskers and fibers in the early literature, whereas nanowires and nanorods with diameters not exceeding a few hundred nanometers are used predominantly in the recent literature, various terms of one-dimensional structures will be used interchangeably, though nanowires in general have a high aspect ratio than that of nanorods. Alternatively, nanowires can be defined as structures that have a thickness or diameter constrained to tens of nanometers or less and an unconstrained length. At these scales, quantum mechanical effects are important, which coined the term "quantum wires". Many different types of nanowires exist, including metallic (e.g., Cu, Ni, Pt , Au), semiconducting (e.g., Si, InP, CdSe , GaN, etc.), and insulating (e.g., SiO_2, TiO_2) [8]. Typical nanowires exhibit aspect ratios (length-to-width ratio) of 1000 or more. As such they are often referred to as one-dimensional (1-D) materials. Nanowires have many interesting properties that are not seen in bulk or 3-D materials. This is because electrons in nanowires are quantum confined laterally and thus

occupy energy levels that are different from the traditional continuum of energy levels or bands found in bulk materials. Different techniques can be used to prepare nanowires:

- **Spontaneous growth:**
  a. Evaporation condensation
  b. Dissolution condensation
  c. Vapor-Liquid-Solid growth (VLS)
  d. Stress induced re-crystallization
- **Template-based synthesis:**
  a. Electrochemical deposition
  b. Electrophoretic deposition
  c. Electrospray
  d. Colloid dispersion, melt, or solution filling
  e. Sol-gel synthesis
  f. Pressure Injection Technique
- **Electrospinning**
- **Lithography**

Spontaneous growth, template-based synthesis and electrospinning are considered as a bottom-up approach, whereas lithography is a top-down technique. Spontaneous growth commonly results in the formation of single crystal nanowires or nanorods along a preferential crystal growth direction depending on the crystal structures and surface properties of the nanowire materials. Template-based synthesis mostly produces polycrystalline or even amorphous products. All the above techniques are used for the preparation of one-dimensional nanostructural materials.

1.2.1 Metal Nanowires

The synthesis of 1D metal nanostructure with high aspect ratios can be directly achieved by electrochemical replication of the cylindrical pores of non-conductive porous membranes. The method has been employed to prepare a variety of metal nanorods and nanowires including zinc , indium , silver ,gold , copper , platinum , palladium , bismuth , nickel , lead , antimony , cobalt and iron . Owing to the direct electrodeposition, their lengths are theoretically proportional to the amount of negative charge passed through the system according to Faraday's law. Compared to the nanorods and nanowires, the synthesis of nanotubes is a challenge for templated electrosynthesis. Most metal nanostructures obtained by templated electrodeposition are polycrystalline. Pulsed electrodeposition has been used to fabricate Cu, Pb, Bi, Ag and Sb single crystal nanowires. An effective method toprepare Ag, Au and Cu single crystal nanowires by templated electrodeposition via a two-dimensional layer by layer nucleation and growth mechanism They employed a lower overpotential, an elevated temperature and a gelatine additive to assist the growth of single crystal noble metal nanowires, it is suggested the conditions employed promote surface diffusion of atoms and thus favours the growth of existing crystal nuclei . However, single crystal growth by electrodeposition is still a great challenge for high melting point metals such as Co, Ni, Rh and Pt. Thermal processing of metal nanowires grown by templated electrodeposition has been used to fabricate metal oxide nanowires.

1.2.2 Semiconductor Nanowires

Deposited CdSe into AAO and track etched polycarbonate membranes using a cyclic voltammetric technique in an aqueous plating solution containing $CdSO_4$, H_2SO_4 and SeO_2.Using a similar method AgTe was electrosynthesised in AAO templates. ZnO

nanowires were produced within AAO templates by applying a cathodic current in an aqueous zinc nitrate solution. They carried out electrodeposition in a DMSO electrolyte solution containing $ZnCl_2$ and oxygen and achieved ZnO nanowires with better crystallinity. We have demonstrated the controlled electrosynthesis of ZnO nanorods within track etched polycarbonate membranes. In the presence of zinc ions, electrosynthesis at 22 ◦C *via* the reduction of hydrogen peroxide yielded polycrystalline zinc oxide nanorods. When electrodeposition was carried out at 90 ◦C, by reducing nitrate ions, single crystal zinc oxide nanorods were obtained. The growth direction of the single crystal ZnO rods obtained at 90 ◦C was perpendicular to the plane. We obtained nanotubes when the electrodeposition of SnO_2 was performed within the polymer templates

1.3 Properties of Nanowires

1.3.1 Optical properties

They demonstrated colours for Au nanoparticles electroplated into the alumina template membrane, ranging from red to purple to blue depending on the diameter of the particles.
A blue shift of the maximum extinction wavelength was observed for both Au and Ag nanoparticles as the particle aspect ratio increasesHigh contrast in reflectivity between Au and Ag segments has been observed optically in Au–Ag striped nanowires. Furthermore, a third metal can be differentiated at intermediate reflectivity, which makes these materials very attractive for information storage.

1.3.2. Electronic Properties

It has been predicted that for nanomaterials electrical resistance will be highly dependent on particle size. In the absence of a magnetic field, negative temperature coefficient of resistance (TCR), i.e., the electrical resistance increases as temperature decreases, have

been observed in measurements on polycrystalline or single-crystal bismuth nanowires generated by templated electrodeposition. However, in bulk Bi, the TCR is metallic-like, i.e., an increase in resistance with increasing temperature. This indicates that Bi nanowires undergo a semimetal-to-semiconductor transition due to 2D quantum confinement effects. The TCR of Bi depends on the carrier concentration and mobility, which have opposite temperature dependence. With an increase of temperatures, the carrier concentration increases, whereas the carrier mobility decreases, leading to a negative and a positive TCR, respectively. The TCR of a Bi sample is ultimately determined by the competition between these two opposing effects. In the case of nanowires, the finite-size effect means that the electron–phonon scattering and electron-boundary scattering limit the carrier mobility and carrier concentration dominates the TCR. The current-voltage (*I–V)* curves showed the linear and ohmic behaviour for Au segments at room temperature, whereas the *I–V behaviour* of the Ppy segments was linear at room temperature and non-linear at low temperatures, which is characteristic of thermally activated charge transport within conducting polymers.

1.3.3 Magnetic Properties

Giant magnetoresistance (GMR), a very large decrease in the electrical resistance of a material when a magnetic field is applied may occur in structures composed of alternating magnetic and non-magnetic metal layers. Pulsed electrodeposition combined with templated synthesis offers a precise technique to produce multisegmented nanowires with GMR. Many nanowires containing magnetic and non-magnetic coupled layers such as Co–Cu, NiFe–Cu, Ni–Cu and Fe–Cu were electrosynthesised in templates and were found to exhibit GMR effects. Using nanowires, GMR with the geometry of the current perpendicular to the plane (CPP) was easily measured. The CPP-GMR measurement of

conventional thin films requires liquid helium temperatures, whereas the CPP-GMR of nanowires can be measured at room temperature.

Advantages of Nanowires:

- ❖ Nanowire devices can be assembled in a rational and predictable because:

a) Nanowires can be precisely controlled during synthesis,

b) Chemical composition,

c) Diameter,

d) Length,

e) Doping/electronic properties

- ❖ Reliable methods exist for their parallel assembly.
- ❖ It is possible to combine distinct Nanowire building blocks in ways not possible in conventional electronics.
- ❖ Nanowires thus represent the best-defined class of nanoscale building blocks, and this precise control over key variables has correspondingly enabled a wide range of devices and integration strategies to be pursued

Application of Nanowire

- ❖ Semiconductor Nanowires have been assembled into a series of electronic electronics devices:
  a) Crossed Nanowire p-n diodes
  b) Crossed Nanowire -FETs
  c) Nanoscale logic gates and computation circuits,
  d) Optoelectronic devices
- ❖ Interconnects for nano electronics
- ❖ Magnetic devices

- ❖ Chemical and biological sensors
- ❖ Biological labels

1.4 Literature Review

The template method has a number of interesting and useful features. First, it is very general and used this method to prepare tubules and fibrils composed of electronically metals, semiconductors, carbons, and other materials [9]. Electrochemical and electroless depositions, chemical polymerization, sol-gel deposition, and chemical vapour deposition have been presented as major template synthetic strategies [10]. The template approach has been extensively investigated in the synthesis of various nanostructures. For example, mesoporous oxides with well-defined and ordered porous structure can be readily synthesized using surfactant or copolymer micelles as templates through sol–gel processing [11-12]. Semiconductor nanowires, nanocrystals, and carbon nanotubes offer many opportunities for the assembly of nanoscale devices and arrays by the bottom-up paradigm. Central to realizing applications through a bottom-up paradigm is the rational control of key nanomaterial parameters, including chemical composition, structure, size, morphology, and doping [13]. Metal-Oxide-Semiconductor CMOS technology is incorporating the nanowire Field-Effect Transistor (FET) concept into post-CMOS processes and has demonstrated substantial advantages. Beyond FETs, new and exciting applications for nanowire memory based on phase change show potential for studying fundamental memory switching at sub-50 nm length scales where the top-down approach tends to damage the materials. Here, we review the most recent progress in both bottom-up and top-down nanowire research for electronic applications [14]. In several studies, electrodeposition in ion track membrane (template method) has been used to create large two dimensional arrays of wires and tubes of different kinds of metals. In particular, copper single crystals were grown in template pores of micrometer size at room temp.

Material	Growth Technique	Reference
Ag	DNA-template, redox	(Braun et al., 1998)
	template, pulsed ECD[a]	(Sauer et al., 2002)
Au	template, EDC[a]	(Hornyak et al., 1997; Zhang et al., 2001)
Bi	stress-induced	(Cheng et al., 2002)
	template, vapor-phase	(Heremans et al., 2000)
	template, ECD[a]	(Piraux et al., 1999)
		(Hong et al., 1999)
		(Yin et al., 2001)
	template, pressure-injection	(Zhang et al., 1998b)
		(Zhang et al., 1999b; Huber et al., 2000)
Bi_2Te_3	template, dc EDC[a]	(Sander et al., 2002)
CdS	liquid-phase (surfactant), recrystallization	(Chen et al., 2002b)
	template, ac EDC[a]	(Xu et al., 2000a)
		(Routkevitch et al., 1996a)
CdSe	liquid-phase (surfactant), redox	(Manna et al., 2000)
	template, ac EDC[a]	(Routkevitch et al., 1996b)
		(Xu et al., 2000b)
Cu	vapor deposition	(Adelung et al., 2002)
	template, ECD[a]	(Gao et al., 2001)
Fe	template, EDC[c]	(Mawiawi et al., 1991)
		(Li and Metzger, 1997)
	shadow deposition	(Sugawara et al., 1997)
GaN	template, CVD[c]	(Cheng et al., 1999)
	VLS[b]	(Huang et al., 2002; Cui et al., 2000)
GaAs	template, liquid/vapor OMCVD[d]	(Berry et al., 1996)
Ge	high-T, high-P liquid-phase, redox	(Heath and LeGoues, 1993)
	VLS[b]	(Wu and Yang, 2000)
	oxide-assisted	(Zhang et al., 2000a)
InAs	template, liquid/vapor OMCVD[d]	(Berry et al., 1996)
InP	VLS[b]	(Duan et al., 2001)
Mo	step decoration, EDC[a]+redox	(Zach et al., 2000)
Ni	template, EDC[a]	(Sun et al., 1999)
		(Nielsch et al., 2001; Yin et al., 2001)
PbSe	liquid phase	(Bashouti et al., 2002)
Pd	step decoration, EDC[a]	(Favier et al., 2001)
Se	liquid-phase, recrystallization	(Gates et al., 2002a)
	template, pressure injection	(Huber et al., 1994)
Si	VLS[b]	(Cui et al., 2001a)
	laser-ablation VLS[b]	(Morales and Lieber, 1998)
	oxide-assisted	(Wang et al., 1998b)
	low-T VLS[b]	(Sunkara et al., 2001)
Zn	template, vapor-phase	(Heremans et al., 2002)
	template, EDC[a]	(Li et al., 2000b)
ZnO	VLS[b]	(Yang et al., 2002)
	template, ECD[a]	(Zheng et al., 2002; Li et al., 2000b)

[a] Electrochemical deposition
[b] Vapor-liquid-solid
[c] Chemical vapor deposition
[d] Organometallic chemical vapor deposition

Table 2: The selected synthesis of nanowires by template assisted technique

by using commercial baths and reverse pulse plating in ultrasonic fields [15]. This technique for the fabrication of copper microstructures having high aspect ratio Effect of over-potential on the surface morphology of electrodeposited copper micro-cylinders [16]. The size or dimensions of the pores depend upon different factors viz. the nature and energy of the incident ions, the target material, etching conditions etc. [17]. Arrays of metal like Cu, Ni nanowires are obtained by electrodeposition in porous templates such as anodic aluminum oxide (AAO) films and nuclear track membranes [18-20]. CdSe nanowires have been produced by direct current (dc) as well as alternating current electrodeposition into the pores of Anodic alumina membrane(AAM) using $3CdSO_4.8H_2O$ and 0.1 Na_2SeO_3. The deionized water was used for preparing the solution [21, 22]. The cation-exchange can be employed to transform one chalcogenide semiconductor into another one with feature sizes on the scale of 30 nm [23, 24]. Self-aligned and well-ordered CdSe nanowires of diameter 250-300 nm have been grown by dc electrochemical deposition using porous anodic alumina templates. The nanowires are found to be crystalline at an elevated growth temperature. UV-visible absorptions spectra revealed a band-gap 1.75eV, which is near to the bulk band gap value of CdSe. The photoluminescence spectrum shows the defect related emission due to the Se vacancies in the nanowires [25]. The Ag/ZnO nano-heterojunctions were synthesized by an electrochemical route. The optical absorption spectroscopy and photoluminescence studies reveal the reaction mechanism at the junction [26]. The Cu–Se Heterojunctions have been fabricated using AAM templates via template synthesis that provides a simple route to the fabrication of metal–semiconductor heterojunctions. The peak-to-valley current ratio decreases with reductionin the diameter of the diodes at room temperature and this reduction is caused by thermally activated surface current [27]. The effects of thermal annealing on the I–V characteristics of Cu–Se resonant tunneling diodes of

diameter size of 100 nm synthesized through the template-based synthesis technique [28]. Nanojunctions of Ag–Cu_2O and Ag–ZnO have been produced by electrodeposition followed by oxidation within anodic aluminium oxide membranes having pores with diameter, 20nm. Voltage–current characteristics have been delineated over the temperature range373–573 K. These show rectification behavior [29]. Synthesis of metal-CdSe-metal nanowires by electrochemical replication of AAO, dissolving the template yields a colloidal suspension of free-standing nanowires. The end-on junction between the semiconductor and the metal makes it possible to align these nanowires between metal contact pads and to make contact exclusively to the metal segments [30].

CHAPTER 2

Materials and Characterization

2.1 Properties of Copper and Cadmium Selenide

The II-IV compound semiconductors like, CdO, CdSe, CdS, CdTe, ZnO, ZnS, ZnSe, ZnTe etc. have been the subject of extensive research both in fundamental studies and for potential applications in devices. The broad range of band gap and lattice constants available from these materials, and the unique phenomena they exhibit, make them attractive for a wide range of application such as infra-red lasers and detectors , blue – green lasers, light emitting diodes, nonlinear optical materials, magneto-optical devices and radiation detectors. The physical and structural properties of copper and cadmium selenide are given below in Table 1.

Properties	Copper	Cadmium Selenide
Chemical formula	Cu	CdSe
Crystal system	Face-centered cubic	Wurtzite
Molar mass	63.546 g/mol	191.37 g/mol
Density	8.02 g/cm^3	5.816 g/cm^3
Melting point	1084.62 °C	1268 °C
Work function	4.7 eV	2.5eV

TABLE 1: Properties of Copper and Cadmium Selenide.

2.2 Template-Assisted Synthesis

The template-assisted synthesis of nanowires is a conceptually simple and intuitive way to fabricate nanostructures. These templates contain very small cylindrical pores or voids within the host materials, and the empty spaces are filled with the chosen material, which adopts the pore morphology, to form nanowires. Template-based synthesis of nanostructured materials is a very general method and can be used in fabrication of nanorods, nanowires and nanotubules of polymers, metals, semiconductors and oxides [32]. For quick reference, examples of typical nanowires that have been synthesized and stud-ied are listed in Table 2.2. In template-assisted synthesis of nanostructures, the chemical stability and mechanical properties of the template, as well as the diameter, uniformity and density of the pores are important characteristics to consider [33].

2.3 Types of Templates

The various types of templates with nanosized channels have been explored for the template growth of nanorods, nanofibrils and nanotube. The most commonly used and commercially available templates are anodic alumina oxide (AAO) membrane [34], radiation track-etched polycarbonate membranes [35] .Other membranes have also been used as templates such as nanochannel array glass [36], radiation track-etched mica, and mesoporous materials [37], porous silicon by electrochemical etching of silicon wafer [38], zeolites [39], carbon nanotubes[40] and DNA [41]. The AAO membranes with uniform and parallel porous structure are made by anodic oxidation of aluminum sheet in solutions of sulfuric, oxalic, or phosphoric acid. The pores are arranged in a regular hexagonal array and densities as high as 10^{11} pores/cm^2 can be achieved. Pore size ranging from l0 nm to 100 μm can be created [41]. The polycarbonate membranes are

made by bombarding a polycarbonate sheet, with typical thickness ranging from 6-20 μm, with nuclear fission fragments to create damage tracks, and then chemically etching these tracks into pores. In radiation track etched membranes, pores have a uniform size as small as 10 nm, though randomly distributed. The pore densities can be as high as 10^9pores/cm^2 [34]. In addition to the desired pore or channel size, morphology, size distribution and density of pores, template materials must meet certain requirements. First, the template materials must be compatible with the processing conditions. For example an electrical insulator is required for a template to be used electrochemical deposition. Except for the template directed synthesis, template materials should be chemically and thermally inert during the synthesis. Secondly, depositing materials or solution must wet the internal pore walls. Thirdly, for the synthesis of nanorods or nanowires, the deposition should start from the bottom or one end of the template channels and proceed from one side to another. Inward growth may result in the pore blockage, so that should be avoided in the growth of "solid" nanorods or nanowires. Kinetically, enough surface relaxation permits maximal packing density, so a diffusion limited process is preferred. Other considerations include the easiness of release of nanowires or nanorods from the templates and of handling during the experiments [41]. In our case we used AAO membrane as template for synthesis of Cu-CdSe-Cu nanowires heterojunctions.

2.3.2 Anodic Aluminum Oxide

The AAO membranes with uniform and parallel porous structure are obtained by anodic oxidation of aluminum metal in solutions of sulfuric, oxalic, or phosphoric acid. The dimensions of the pores are tunable in the range of four to several hundred nanometers, which render it an ideal template material for creating arrays of cylindrical nanostructures as shown in Figure 2.3. Unlike the track-etch membranes, the pores in AAO templates

have little or no tilt with respect to the surface normal resulting in an isolating, non connecting pore structure Pore densities as high as 10^{11} cm^{-2} [35] can be obtained, and typical membrane thickness can range from 10 to 100μm. The figure 2.1 shows the SEM micrograph of AAO. The AAO membranes have porosity of 40% to 65% .

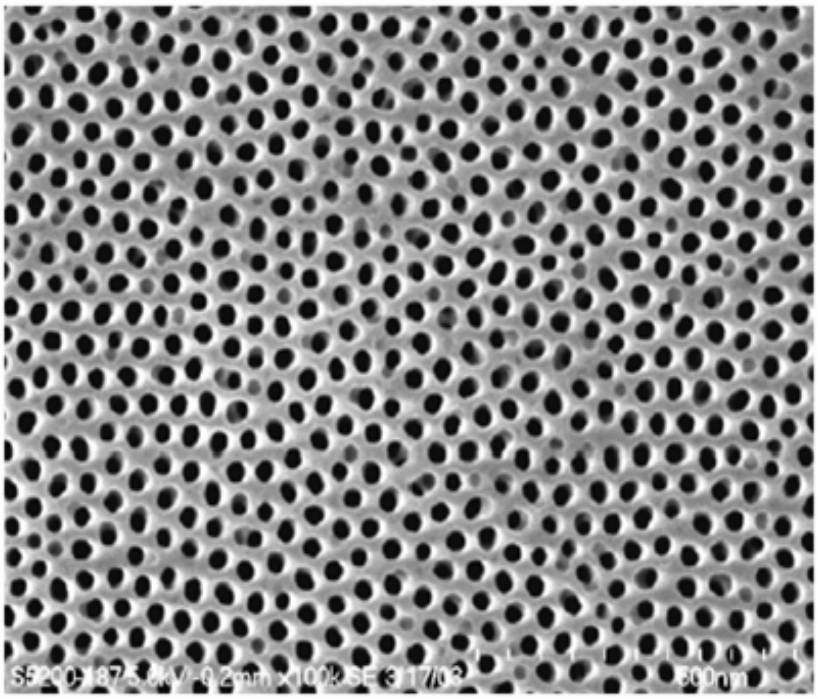

Figure1.2: The SEM micrograph of AAO template

2.4 Electrochemical Deposition

The electrodeposition of a material within the pores of the matrix is preceded by coating one face of the template with a metal film and using this metal film as a cathode for electroplating. The volume of the pore is continuously filled up beginning from the pore bottom. Thus, the length of a nanostructure can be controlled by varying the amount of material deposited. The schematic diagram 1.3 showing growth of nanowires and time versus current behavior [32]. The process was carried out at constant potential so that the deposition could be monitored from the current response . The electrochemistry of the template synthesis of nanowires was studied by comparing the potentiostatically

measured current–time characteristics obtained during wire growth for different pore dimensions and a pore-size dependence of the diffusion co-efficient for the metal ions was found [32].

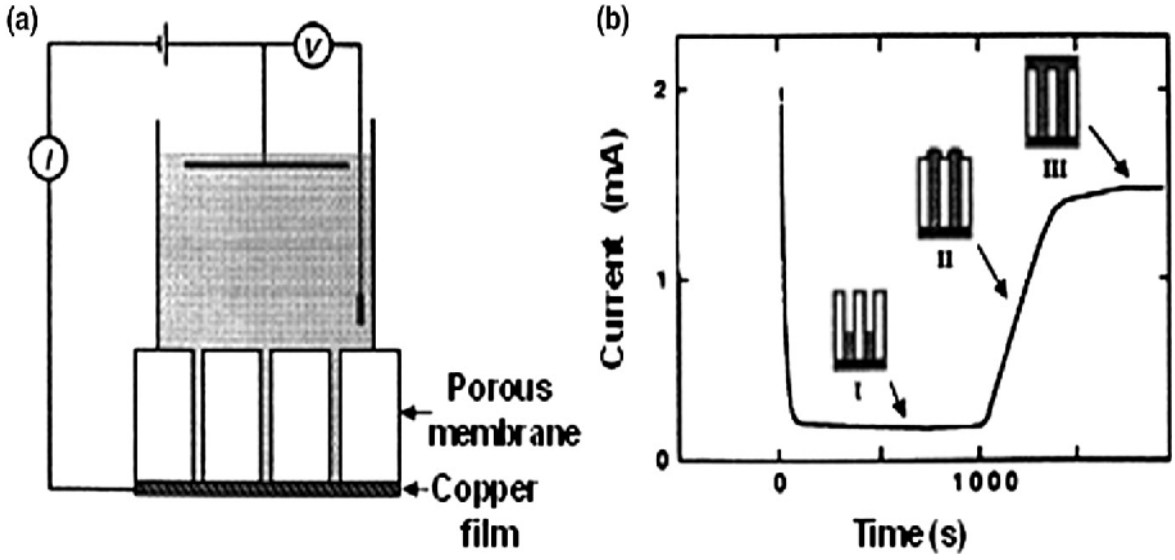

Figure 1.3: The schematic diagram showing electrodeposition of nanowires and time versus current behavior.

The electrochemical deposition, also known as electrodeposition, involves oriented diffusion of charged reactive species through a solution when an external electric field is applied, and reduction of the charged growth species at the growth or deposition surface which also serves as an electrode. In industry, electrochemical deposition is widely used in making metallic coatings in a process known as electroplating [42]. In general, this method is only applicable to electrical conductive materials such as metals, alloys, semiconductors, and electrically conductive polymers and oxides. After the initial deposition, the electrode is separated from the depositing solution by the deposit and the electrical current must go through the deposit to allow the deposition process to continue. When deposition is confined inside the pores of template membranes, nanocomposites are produced. If the template membrane is removed, nanorod or nanowire arrays are

prepared. However, when the deposition occurs along the wall surface of the pore channels, nanotubes would form.

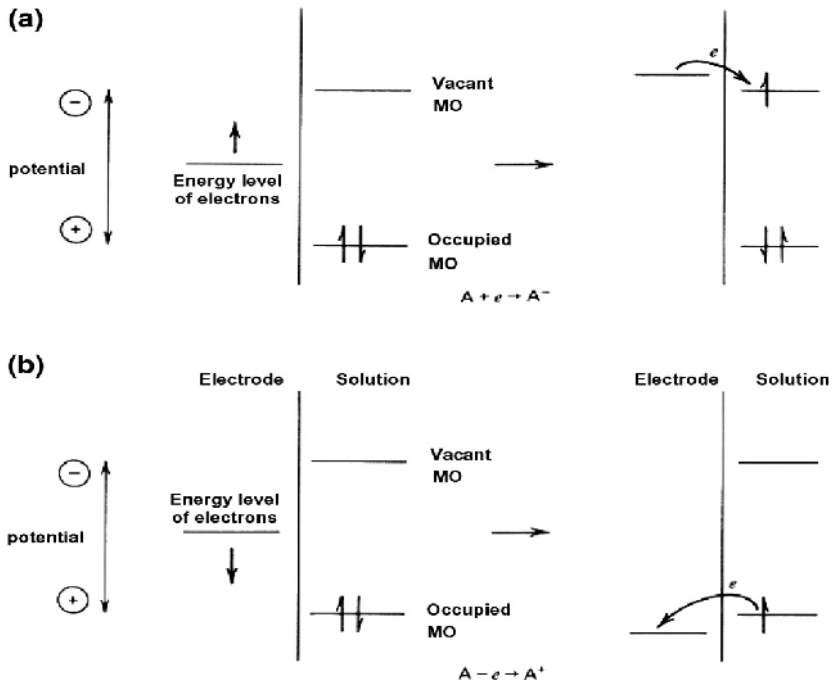

Figure 1.4: Representation of (a) reduction and (b) oxidation process of a species A in solution. The molecular orbitals (MO) of species A shown are the highest occupied MO and the lowest vacant MO.

When a solid immerses in a polar solvent or an electrolyte solution, surface charge will develop. The electrode potential is described by the Nernst equation:

$$E = E_0 + \frac{RT}{n_i F}\ln(a_i)$$

where E_0 is the standard electrode potential, or the potential difference between the electr -ode and the solution, when the activity, a_i of the ions is unity, F the Faraday's constant, R, the gas constant, and T, temperature. When the electrode potential is more negative

(higher) than the energy level of vacant molecular orbital in the electrolyte solution, electrons will transfer from the electrode to the solution, accompanied by electrolyte reduction as shown in figure 1.4 (a) [43]. If the electrode potential is more positive (lower) than the energy level of the occupied molecular orbital, the electrons will transfer from the electrolyte solution to the electrode, accompanied by electrolyte oxidation, as illustrated in figure 1.4 (b) [43]. The reactions stop when the equilibrium is achieved. When an external electric field is applied between two dissimilar electrodes, charged species flow from one to another electrode, and electrochemical reactions occur at both electrodes. This process is called electrolysis, which converts electrical energy to chemical potential. The system used for the electrolysis process is called electrolytic cell. In such a system the electrode connected to the positive side of the power supply is an anode, at which an oxidation reaction takes place, whereas the electrode connected to the negative side of the power supply is a cathode, at which a reduction reaction proceeds, accompanied by deposition. Therefore, electrolytic deposition is also called cathode deposition, but most commonly referred to as electrochemical deposition or electrodeposition. The growth of nanowires of conductive materials in an electric field is a self-propagating process [43]. Once the small rods form, the electric field and the density of current lines between the tips of nanowires and the opposing electrode are greater than that between two electrodes due to a shorter distance. The growth species keep on depositing onto the tip of nanowires, resulting in continued growth. To better control the morphology and size, templates with desired channels are used to guide growth of nanowires. The figure 1.3 illustrates the common setup for the template-based growth of nanowires [44]. The template is attached onto the cathode, which is brought into contact with the deposition solution. The anode is placed in the deposition solution, parallel to the cathode. When an electric field is applied, cations diffuse through the

channels toward and deposit on the cathode, resulting in the growth of nanowires inside the template. This figure also schematically shows the current density at different deposition stages when a constant electric field is applied. The current does not change significantly until the pores are completely filled, at which point the current increases rapidly due to the improved contact with the electrolyte solution. The current saturates once the template surface is completely covered.

2.5 Characterization Techniques

The characterization of materials regarding determination of elemental composition, estimation of trace impurities, structural analysis, morphological analysis, identification of crystalline phases and information on crystal defects plays an important role for the quality control and development of advanced materials and their use in precision devices. The nanowire heterojunctions have been characterized by their structural, compositional, morphological and electrical transport properties. The techniques used include X-Ray Diffraction (XRD), Scanning Electron Microscopy (SEM), Energy Dispersive X-ray Spectroscopy (EDAX) and Electro-Source Meter for current voltage (I-V) measurement.

2.5.1 Structural and Phase Analysis by XRD

X-ray diffraction is a versatile, non-destructive method that reveals detailed information about the chemical composition, crystallographic and micro structure of all types of natural and manufactured materials. It is a valuable tool for the research and development of advanced materials. It provides information on structure, phase, preferred crystal orientations (texture) and other parameter such as average grain size, crystallinity, strain, crystal defects and crystallites size. The interaction of x-rays with sample creates secondary "diffracted" beams of x-rays related to interplanar spacing's in the crystalline powder according to a mathematical relation called Bragg's Law [45]:

$$n\lambda = 2d \sin\theta$$

where **n** is an integer, **λ** is the wavelength of the X-rays, **d** is the interplanar spacing generating the diffraction and **θ** is the diffraction angle. X-ray diffraction is based on the

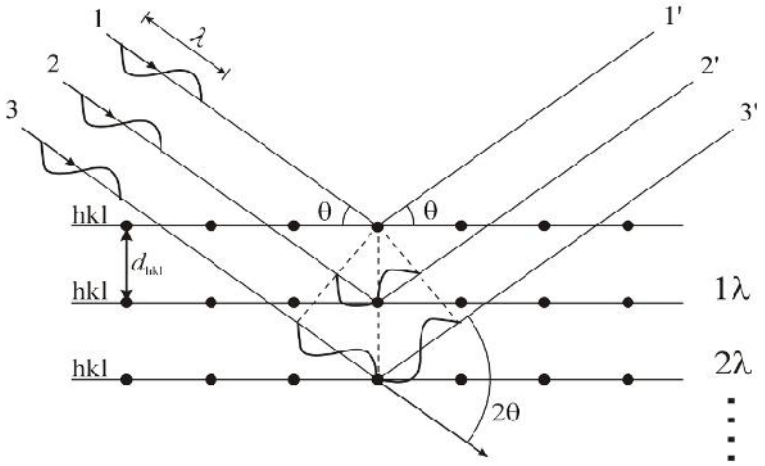

Figure 1.5: Schematic diagram of Bragg's diffraction from a set of parallel planes

constructive interference of monochromatic X-rays and a crystalline sample. These x-rays are generated by a cathode ray tube, filtered to produce monochromatic radiation, collimated to concentrate, and directed toward the sample. The figure 1.5 shows schematic of Bragg's diffraction from a set of parallel planes. The interaction of the incident rays with the sample produces constructive interference when conditions satisfy Bragg's law. This law relates the wavelength of electromagnetic radiation to the diffraction angle and the lattice spacing in a crystalline sample. These diffracted x-rays are then detected, processed and counted. The figure 1.7 shows experimental set for XRD. The geometry of x-ray diffractometer is such that the sample rotates in the path of the collimated x-ray beam at an angle θ while the x-ray detector is mounted on an arm to collect the diffracted x-rays and rotates at an angle of 2θ. The lattice should be attained due to the random orientation of the powdered material. All diffraction methods are based on generation of X-rays in an X-ray tube. These X-rays are

Figure 1.6: The PANalytical's X-ray diffractometer.

directed at the sample, and the diffracted rays are collected. A key component of all diffraction is the angle between the incident and diffracted rays.

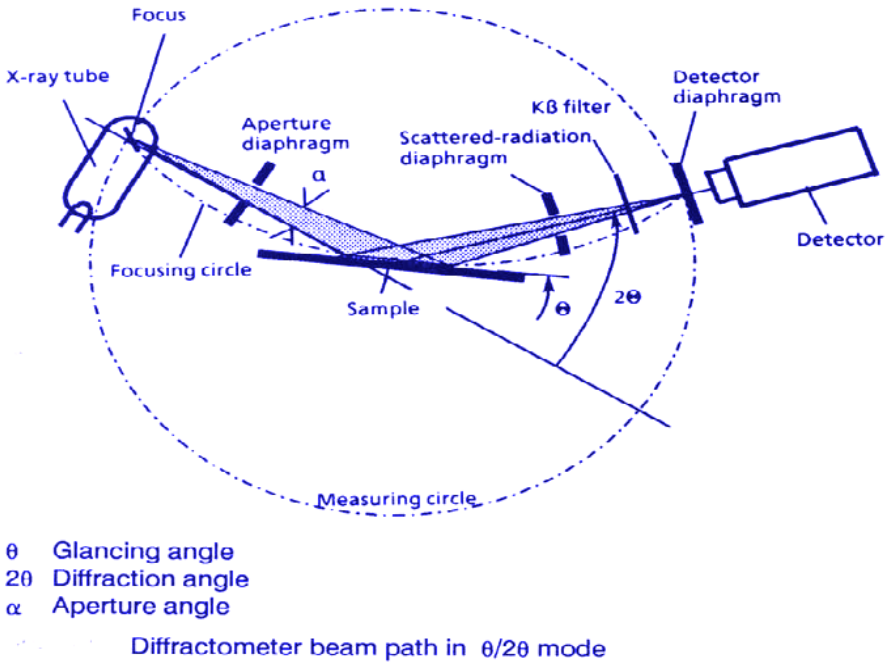

Figure 1.7: The experimental set-up for x-ray diffractometer.

Uses of X-ray diffraction

- The degree of crystallinity of the phases.

- The determination of layer and coating thicknesses, densities and roughnesses.
- Identification of single-phase materials – minerals, chemical compounds, ceramics or other engineered materials.
- Identification of multiple phases in microcrystalline mixtures (i.e., rocks)
- Determination of the crystal structure of identified materials
- Identification and structural analysis of clay minerals
- Recognition of amorphous materials in partially crystalline mixtures
- Crystallographic structural analysis and unit-cell calculations for crystalline materials.
- Quantitative determination of amounts of different phases in multi-phase mixtures by peak-ratio calculations.
- Quantitative determination of phases by whole-pattern refinement.
- Determination of crystallite size from analysis of peak broadening.
- Determine of crystallite shape from study of peak symmetry.
- Study of thermal expansion in crystal structures using in-situ heating stage.
- Analysis of epitaxial layers, heterostructures and superlattice system

2.5.2 Scanning Electron Microscopy

The scanning electron microscope (SEM) is a type of electron microscope that images the sample surface by scanning it with a high-energy beam of electrons in a raster scan pattern. The SEM is a microscope that uses electrons instead of light to form an image. The electrons interact with the atoms that make up the sample producing signals that contain information about the sample's surface topography, composition and other properties such as electrical conductivity. The scanning electron microscope has many advantages over traditional microscopes like, large depth of field, higher resolution (~ 1

nm) [46]. In a typical SEM, as shown in figure 1.8 an electron beam is thermionically emitted from an electron gun fitted with a tungsten filament cathode. Tungsten is normally used in thermionic electron guns because it has the highest melting point and lowest vapor pressure of all metals.

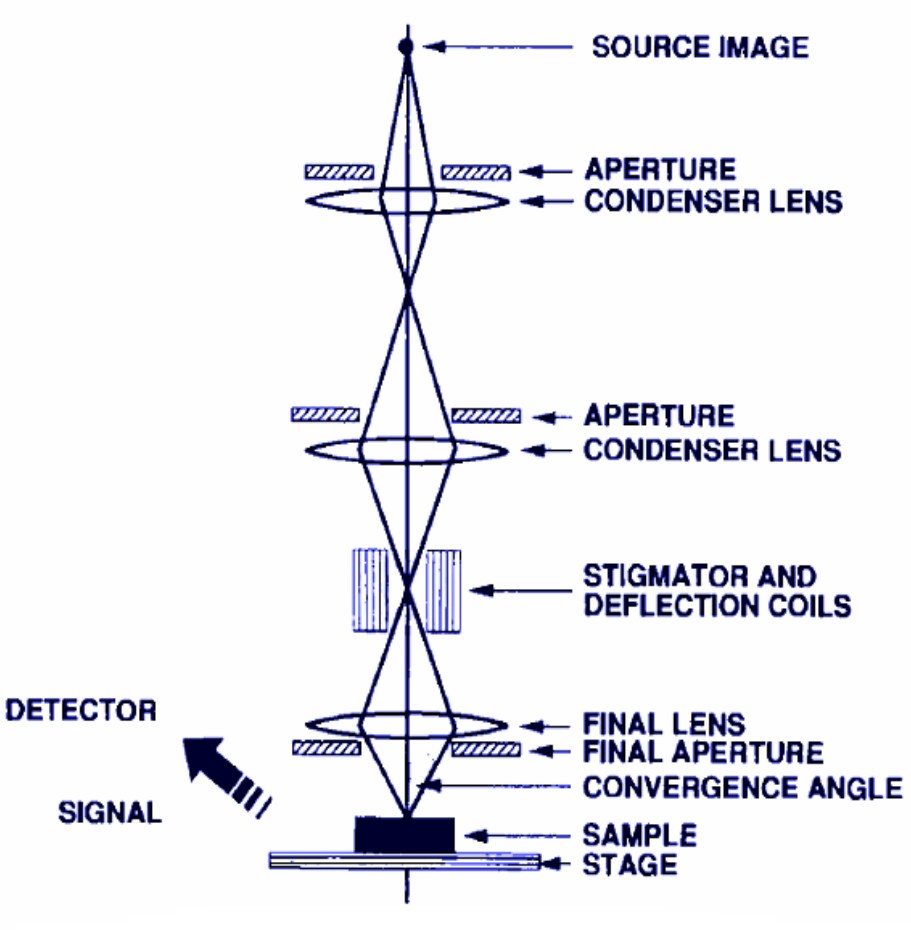

Figure 1.8: The basic experimental set up of SEM

The electron beam, which typically has an energy ranging from a few hundred eV to 40 keV, is produced at the top of the microscope by an electron gun. The beam passes through pairs of scanning coils or pairs of deflector plates in the electron column, typically in the final lens, which deflect the beam in the *x* and *y* axes so that it scans in a raster fashion over a rectangular area of the sample surface. Once the beam hits the sample, electrons and x-rays are ejected from the sample. The detectors collect these x-

rays, backscattered electrons, and secondary electrons and convert them into a signal that is sent to a screen similar to a television screen. This produces the final image.

Figure 1.9: The JEOL JSM-6510 LV Scanning Electron Microscope.

.

All samples must also be of an appropriate size to fit in the specimen chamber and are generally mounted rigidly on a specimen holder called a specimen stub. For conventional imaging in the SEM, specimens must be electrically conductive, at least at the surface, and electrically grounded to prevent the accumulation of electrostatic charge at the surface. Two important reasons for coating, even when there is more than enough specimen conductivity to prevent charging, are to maximize signal and improve spatial resolution, especially with samples of low atomic number (Z). The improvement in resolution arises because in low-Z materials such as carbon, the electron beam can penetrate several micrometers below the surface, generating signals from an interaction volume much larger than the beam diameter and reducing spatial resolution. Coating with a high-Z material such as gold maximizes secondary electron yield from within a surface layer a few nm thick, and suppresses secondary electrons generated at greater depths, so

that the signal is predominantly derived from locations closer to the beam and closer to the specimen surface than would be the case in an uncoated, low-Z material.

2.5.3 Energy Dispersive X-ray Spectroscopy

The energy dispersive x-ray spectroscopy, is an analytical technique that uses characteristic x-ray radiation for compositional analysis. A major advantage of the energy-dispersive spectrometer is that it can be positioned very close **to** the sample and can present a large solid angle for the collection of emitted x-rays. The figure 3.3 shows the schematic of principle of EDAX analysis and different process involve when x-ray interact with sample. It based on the investigation of a sample through interactions between electromagnetic radiation and matter, analyzing x-rays emitted by the matter in response to being hit with charged particles. To stimulate the emission of characteristic x-rays from a specimen, a high energy beam of charged particles such as electrons or protons, or a beam of x-rays, is focused into the sample being studied. At rest, an atom within the sample contains ground state (or unexcited) electrons in discrete energy levels or electron shells bound to the nucleus. The incident beam may excite an electron in an inner shell, ejecting it from the shell while creating an electron hole where the electron was. An electron from an outer, higher-energy shell then fills the hole, and the difference in energy between the higher-energy shell and the lower energy shell may be released in the form of an x-ray (as shown in figure 1.10). The number and energy of the X-rays emitted from a specimen can be measured by an energy dispersive spectrometer. As the energy of the x-rays is characteristic of the difference in energy between the two shells, and of the atomic structure of the element from which they were emitted, this allows the elemental composition of the specimen to be measured [47]. There are three modes of analysis commonly used: spectrum acquisition; spatial distribution, or dot, mapping of the

elements; and elemental line scans. The figure 1.11 shows The NORAN's SIX Model 300 EDAX attached with JEOL 6500 SEM used for analysis.

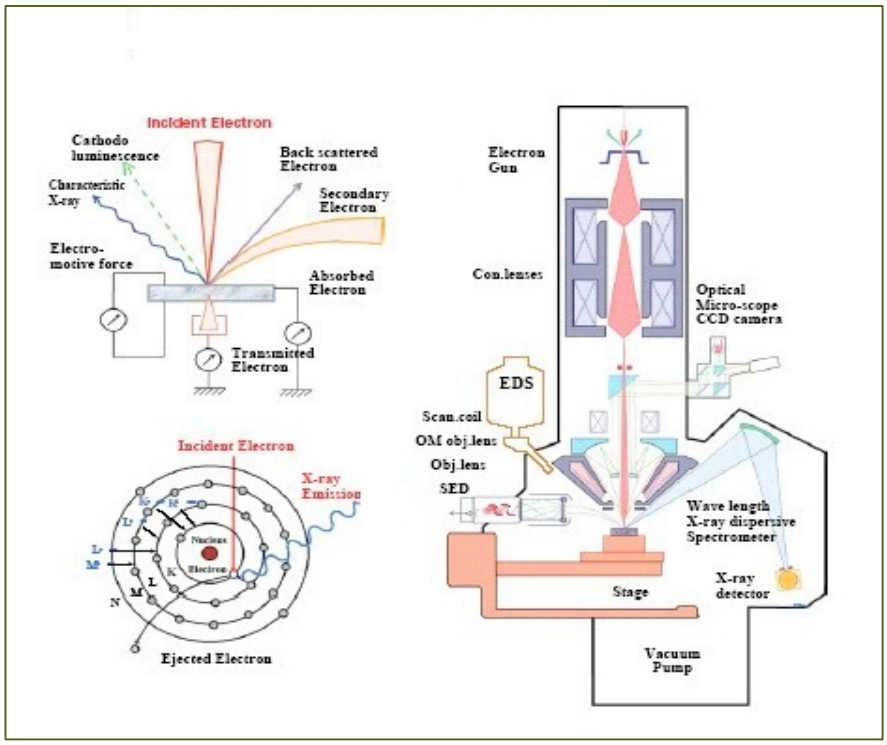

Figure 1.10: The Illustration of the principle of EDAX

The energy of the x-ray photon depends on the element of which the electron was a part, as well as the initial and final states of the electron making the transition. These energies are predictable. The x-ray producing transitions are commonly grouped into categories based on the initial and final states of the electron. These transitions are labeled as XJ, with X denoting the final state shell of the electron (K for n = 1, L for n = 2, M for n = 3, and so on), and J indicating how many shells above the final state the electron transitioned from (i = α, β, γ, . . for 1, 2, 3, … respectively). For example, L_{β} would indicate that the electron transitioned to the n = 2 shell, from 2 shells above (n = 4). The

typically Kα x-ray transitions are the strongest emission lines seen, which occur when an electron transitions from the $n = 2$ shell to the $n = 1$ shell. The energy given off (in the form of an X-ray photon) can calculated as, equation

$$E_{K_\alpha} = E_0 (Z - 1)^2 \left[\frac{1}{1^2} - \frac{1}{2^2} \right]$$

Where $E_0 = 13.6\ eV$, and Z (an integer ≥ 2) is the atomic number of element. This simplifies to,

$$E_{K_\alpha} = (10.2\ eV)(Z - 1)^2 .$$

Figure 1.11: The NORAN's SIX Model 300 EDAX attached with JEOL 6500 SEM.

Further refinements can be made by taking into account more of the quantum numbers describing the states from which the electrons transition to from, such as the angular momentum and spin, as well as selection rules describing which transitions are allowed.

2.5.4 The Current-Voltage characteristics

The study of electrical transport properties of nanowires is important for nanowire characterization, electronic device applications, and the investigation of unusual transport phenomena arising from one-dimensional quantum effects. Important factors that determine the transport properties of nanowires include the wire diameter, which is important for both classical and quantum size effects, material composition, surface conditions, crystal quality, and the crystallographic orientation along the wire axis for materials with anisotropic materials parameters, such as the efective mass tensor, the Fermi surface, or the carrier mobility [48]. The KEITHLEY source meter, 4200-SCS, attached with ZYVEX S100 Nanomanipulator, with probe size 500 nm, made up of tungsten, was used for collective I–V measurements as shown in figure 1.12. The Keithley 4200-SCS Semiconductor Characterization System combined with the Zyvex Test System is an extremely effective measurement tool for I-V characterization of nanoscale components. With four-point probe capability, 1pA accuracy, and 5nm precision movement, the system offers a unique combination of features that is ideal for nanotechnology and semiconductor characterization. The Zyvex S100 Nanomanipulator is a positioning and testing tool for micro- and nano-scale research and development applications. It accommodates up to four positioners (three-dimensional stages) with 5nm positioner resolution that grasp, move, test, and optimally position micro- and nano-scale samples in SEM. For a four-point measurement on a nanoscale wire or tube, all four positioners of the test system are used. Each positioner controls a single probe. The figure 1.13 illustrates the connections of the Keithley 4200-SCS with the S100. To implement a four-point measurement on nanoscale materials and wires, the outer and inner probes that are closest to each other on the DUT connect to the same Source-Measure Unit (SMU).

The outer probe connects to the force terminal on the SMU and the inner probe connects to the sense terminal on the SMU.

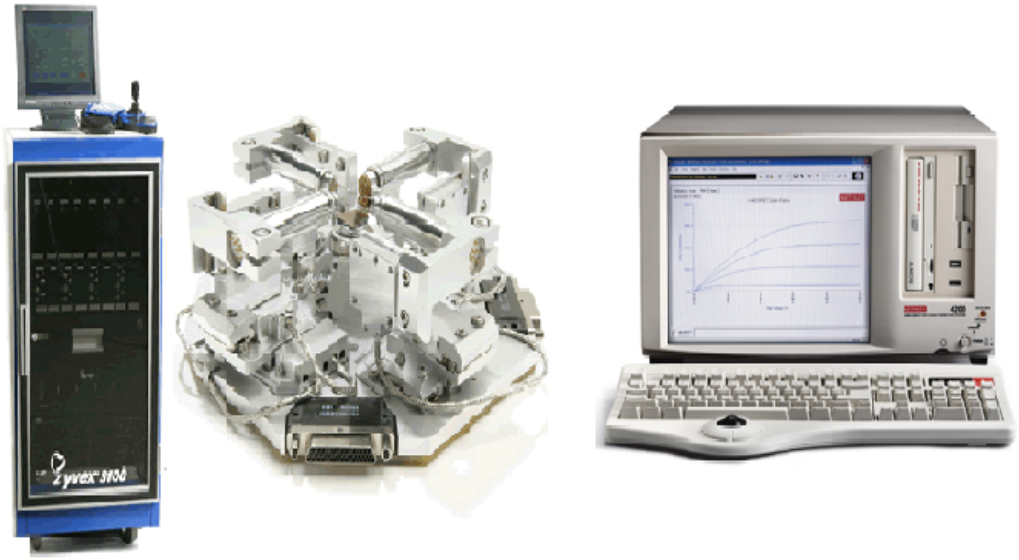

Figure 1.12: The experimental set-up for I-V characterization

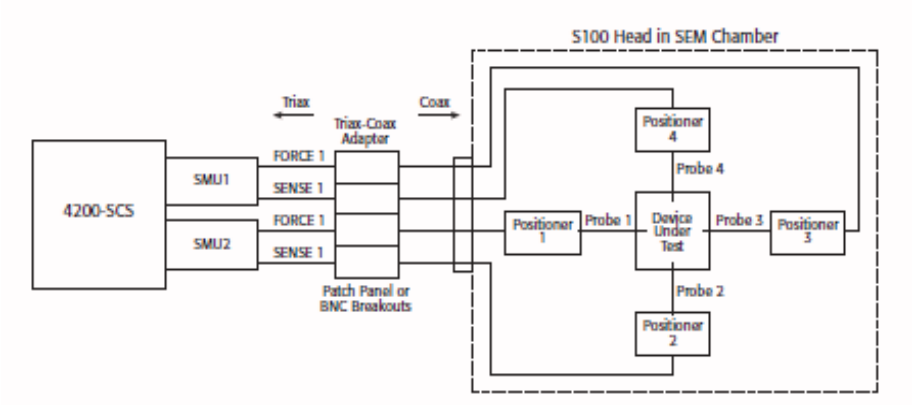

Figure 1.13: The schematic diagram of Zyvex S100 test head with Keithley 4200-SCS

The nano-manipulator and its probes, along with a source-measure unit (SMU), are used to apply a current or voltage stimulus directly to the nanoparticle and measure its

corresponding voltage or current response (figure 3.6). The advantage of electrical source-measure testing is rooted in the fact that a specific SMU measurement mode (source current/measure voltage or vice versa) can be chosen based on the relative Impedance of the material or device under test (DUT) [49].A solution to the problem of two-point measurements that measure the lead and contact resistance along with that of the device under test is the four-wire or "Kelvin" measurement. With Kelvin measurements, a second set of probes is used for sensing. The negligible current flows in these probes; therefore, only the voltage drop across the DUT is measured (see figure 1.14). As a result, resistance measurement or I-V curve generation is more accurate.

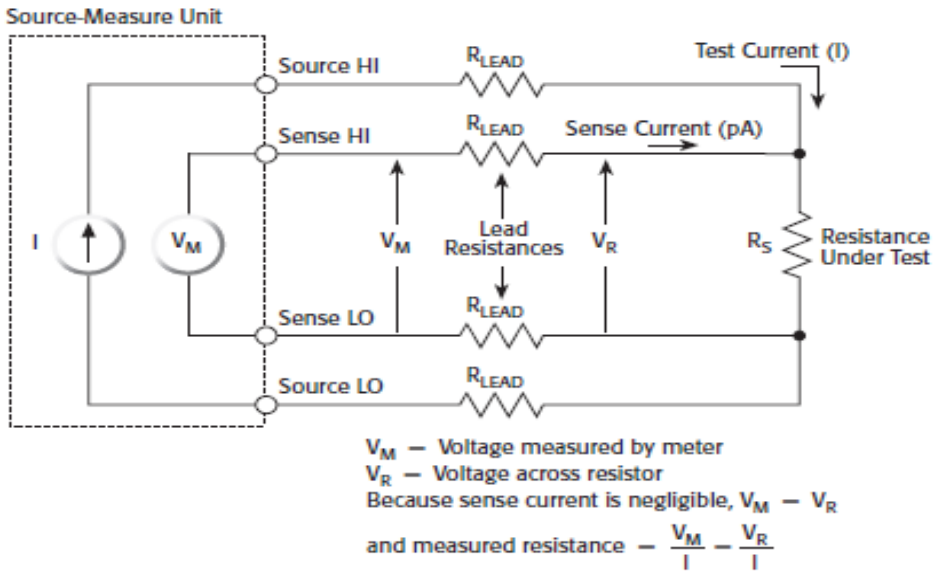

Figure 1.14: The four probe set up for I-V measurement.

CHAPTER 3

Experimental Details

3.1 Introduction

A heterojunction is a junction between two, dissimilar, crystalline material where the crystal structure is continuous across the interface. This type of structure was first envisaged by Preston [50]. A heterojunction is the interface that occurs between two layers or regions of dissimilar crystalline semiconductors. These semiconducting materials have unequal band gaps as opposed to a homojunction. It is often advantageous to engineer the electronic energy bands in many solid state device applications including semiconductor lasers, solar cells and transistors "heterotransistors" to name a few. The combination of multiple heterojunctions together in a device is called a heterostructure although the two terms are commonly used interchangeably. The requirement that each material be a semiconductor with unequal band gaps is somewhat loose especially on small length scales where electronic properties depend on spatial properties. A more modern definition may be to say that a heterojunction is the interface between any two solid state materials including crystalline and amorphous structures of metallic, insulating, fast ion conductor and semiconducting material. In 2000, the physics Nobel Prize was awarded with one half jointly to Herbert Kroemer (University of California at Santa Barbara, California, USA) and Zhores I. Alferov (A.F. Ioffe Physico-Technical Institute, St. Petersburg, Russia) for "developing semiconductor heterostructures used in high-speed and optoelectronics". In the nanowires heterojunction the band energies are dependent on crystal size due to the quantum size effects. This enables band offset engineering in nanoscale heterostructures. It is possible [51] to use the same materials but change the type of junction, say from straddling (type I) to staggered (type II), by changing the size or thickness of the crystals involved. The most common

nanoscale heterostructure system is core\shell CdSe\ZnS which is a straddling gap (type I) offset. In this system the much larger band gap ZnS passivates the surface of the fluorescent CdSe core thereby increasing the quantum efficiency of the luminescence. There is an added bonus of increased thermal stability due to the stronger bonds in the ZnS shell as suggested by its larger band gap. Since CdSe and ZnS both grow in the zincblende crystal phase and are closely lattice matched, core shell growth is preferred. In other systems or under different growth conditions it may be possible to grow anisotropic structures such as the one seen in the image on the right. It has been shown [52] that the driving force for charge transfer between conduction bands in these structures is the conduction band offset. By decreasing the size of CdSe nanocrystals grown on TiO_2, Robel et al. [53] found that electrons transferred faster from the higher CdSe conduction band into TiO_2. In CdSe the quantum size effect is much more pronounced in the conduction band due to the smaller effective mass than in the valence band, and this is the case with most semiconductors. Consequently, engineering the conduction band offset is typically much easier with nanoscale heterojunctions. For staggered (type II) offset nanoscale heterojunctions, photo induced charge separation can occur since there the lowest energy state for holes may be on one side of the junction where as the lowest energy for electrons is on the opposite side. It has been suggested [54] that anisotropic staggered gap (type II) nanoscale heterojunctions may be used for photocatalysis, specifically for water splitting with solar energy. Using heterojunctions in lasers was first proposed [55] in 1963 when Herbert Kroemer, thought of as the father of this field, suggested tha tpopulation inversion could be greatly enhanced by heterostructures. By incorporating a smaller direct band gap material like GaAs between two larger band gap layers like AlAs, carriers can be confined so that lasing can occur at room temperature with low threshold currents. It took many years

for the material science of heterostructure fabrication to catch up with Kroemer's ideas but now it is the industry standard. It was later discovered that the band gap could be controlled by taking advantage of the quantum size effects in quantum well heterostructures. Furthermore, heterostructures can be used as waveguides to the index step which occurs at the interface, another major advantage to their use in semiconductor lasers. Semiconductor diode lasers used in CD & DVD players and fiber optic transceivers are manufactured using alternating layers of various III-V and II-VI compound semiconductors to form lasing heterostructures. When a heterojunction is used as the base-emitter junction of a bipolar junction transistor, extremely high forward gain and low reverse gain result. This translates into very good high frequency operation (values in tens to hundreds of GHz) and low leakage currents. This device is called a heterojunction bipolar transistor (HBT). Heterojunctions are used in high electron mobility transistors (HEMT) which can operate at significantly higher frequencies (over 500 GHz). The proper doping profile and band alignment gives rise to extremely high electron motilities by creating a two dimensional electron gas within a dopant free region where very little scattering can occur.

3.1 Electrdeposition of Nanowires Heterojunctions

The electrochemical deposition technique has attracted increasing attention as a promising alternative for fabricating nanowires heterojunctions. Traditionally, electrochemistry has been used to grow thin films on conducting surfaces. Since electrochemical growth is usually controllable in the direction normal to the substrate surface, this method can be readily extended to fabricate one dimensional or zero dimensional nanostructures, if the deposition is confined within the pores of an appropriate template. In the electrochemical methods, a thin conducting metal film is first coated on one side of the porous membrane to serve as the cathode for electroplating. The

length of the deposited nanowires or nanowires heterojunctions can be controlled by varying the duration of the electroplating process or growth conditions like temperature, pH etc. of solution used. The templated electrosynthesis offers many remarkable advantages over other methods for the synthesis of one-dimensional (1D) nanomaterials and ordered porous materials: (1) template electrodeposition is performed under mild conditions rather than requiring high temperatures, high vacuum or expensive instrumentation [8]; (2) templated electrodeposition has a relatively high growth rate; (3) the morphology of deposited materials is obviously dependent on the shape of template pores; (4) tuning of the template pore size and effective integrated charge passed in electrodeposition can be used to tune the dimensions of the materials obtained; (5) two or more components can be easily deposited into the membrane sequentially to form multisegmented materials [56]. The basic layout of the electrochemical cell used for deposition of nanowires heterojunctions is shown in figure 1.15.

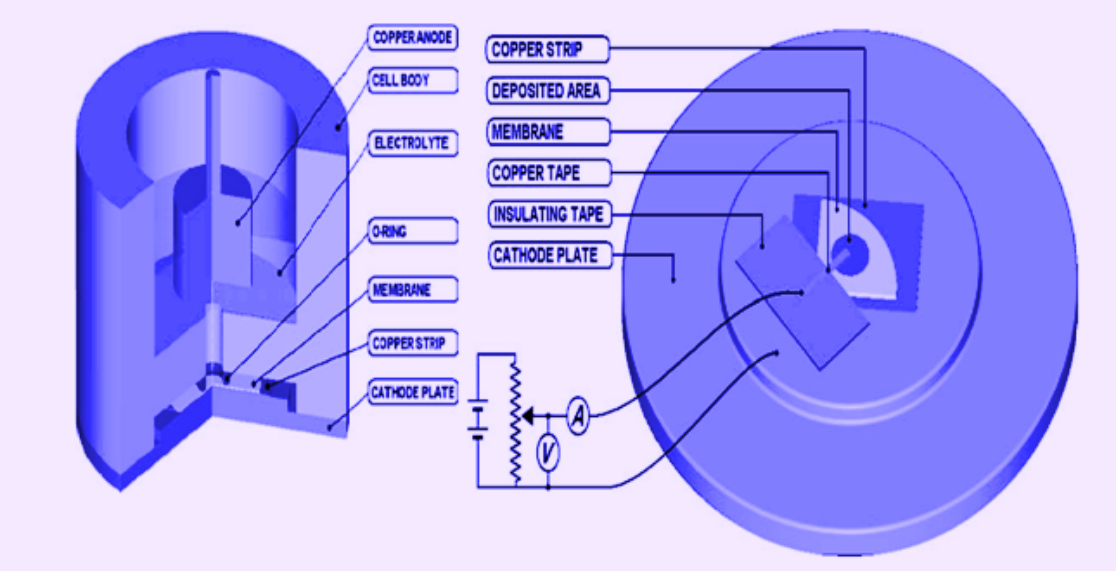

Figure 1.15: The basic layout of electrochemical cell used for deposition of nanowires heterojunction.

By controlling the growth parameter, like temperature of solution used, pH of solution,

the distance between electrodes and the stirring of solution during growth, we can control size, length, and morphology of nanowires heterojunctions.

3.2 Synthesis Strategy

All the chemicals and reagents were of AR grade, were obtained from s.d.fine-chem Ltd, Mumbai, India, and used without further purification. The list of chemical used is given in table 3 .The deionised water was used for preparing solutions. The electrochemical deposition was performed using commercially available templates (Anodisc-25, Whatman, with quoted pore diameters of 100 nm, 300 nm and thickness 60 μm). Before the growth of hetrojunctions, a thin conductive layer of silver was thermally evaporated on one side of the templates for making electrical contact. Two electrode cell, made of perspex, designed in our laboratory, was used. The main parameters controlled during the growth of nanowires heterojunctions were the pH of the solutions, kept at 2.5 using 25% H_2SO_4; the distance between the electrodes, kept at 2 cm; the temperature of solutions and the electrolytes constantly stirred. The template, coated on one side with thin silver layer, was then placed on the cathode plate of the electrochemical cell with the open pores side facing upward. The figure 1.16 shows the schematic diagram of various steps involved in the growth of Cu-CdSe-Cu nanowire hetrojunctions. The Cu, CdSe and Cu have been deposited in the template pores such that the pore length occupied by each of them is in the ratio of 1:6:1. The Cu, CdSe and Cu were deposited, in that sequence, in the template pores, respectively for 2, 12 and 2 minute, to resume maximum possible length of the CdSe segment; Cu on either side is just for electrical connections. First, the electrodeposition of Cu metal was carried out as shown in figure 1.16 (b) by using electrolyte having a composition of 0.5 M $CuSO_4.5H_2O$ and 0.5 ml of 25% dilute H_2SO_4 with pure copper rod as an anode. A potential difference of 2 V (current 0.015 to 0.020 A)

was applied between the electrodes for 2 minute at room temperature (27^{o}C). After this, the electrolyte was drained off and another electrolyte solution of composition 0.5 M $CdSO_4.8H_2O$ and 0.5 M Na_2SeO_3 with 0.5 ml of 25% dilute H_2SO_4 was taken for the deposition of CdSe segment as shown in figure1.16 (c). The deposition was carried out for 12 minute at 2 V (current 0.018 to 0.040 A) and 80ºC temperature with pure cadmium rod as an anode. Finally, the deposition of copper (figure1.16 (d)), using same parameters as mentioned above, was done.

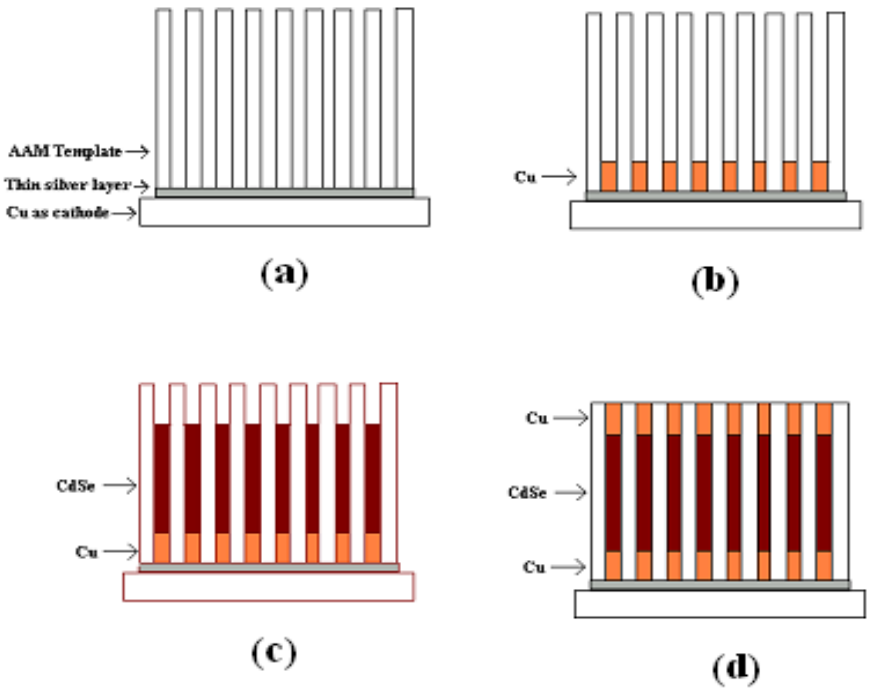

Figure 1.16: Schematic diagram showing various steps involved in growth of Cu-CdSe-Cu nanowires heterojunctions (a) AAM on which one side is coated with silver conductive layer (b) Electrochemical deposition of Cu metal (c) Electrodeposition deposition of CdSe semiconductor (d) electrodeposition of Cu metal (e) and collective I-V characteristics measurement set up.

Once the electrodeposition was over, the electrolyte was drained off. The Cu-CdSe-Cu nanowires heterojunctions were removed from the matrix after dissolving the template in 0.5 M NaOH solution at 27°C for 2 hour, followed by washing several times with deionised water, then with ethanol, and subsequently drying these in hot air oven at ambient temperature for overnight.

S. No	Name Of Chemical	Molecular Formula	Molecular Weight	Grade
1.	Cupric Sulphate	$CuSO_4 .5H_20$	249.68	AR
2.	Sulphric Acid	H_2SO_4	98	AR
3.	Cadmium Sulphate	$3CdSO_4 .8H_2O$	769.54	AR
4.	Sodium Selenite	Na_2SeO_3	172.94	AR
5.	Sodium Hydroxdie	NaOH	40.00	AR
6.	Acetone	$(CH_3)_2CO$	58 .08	AR
7.	Ethanol	C_2H_5OH	48.0	AR

Table 3: The list of chemical used

4.1 X-ray diffraction analysis

The structural and phase analysis of Cu-CdSe-Cu nanowire heterojunctions was performed using X-Ray Diffractometer of PANalytical X'Pert PRO MRD (Netrherland) with CuKα (λ = 1.5418 Å) radiation operated at 45 kV and 40 mA. The high intense beam was focused over a small area (10 mm) of the sample using x-ray lens, and gonio scan was recorded for 2θ value from 10^{o} to 90^{o}. XRD pattern of Cu-CdSe-Cu nanowire heterojunctions embedded in an AAO template is shown in figure 1.17.

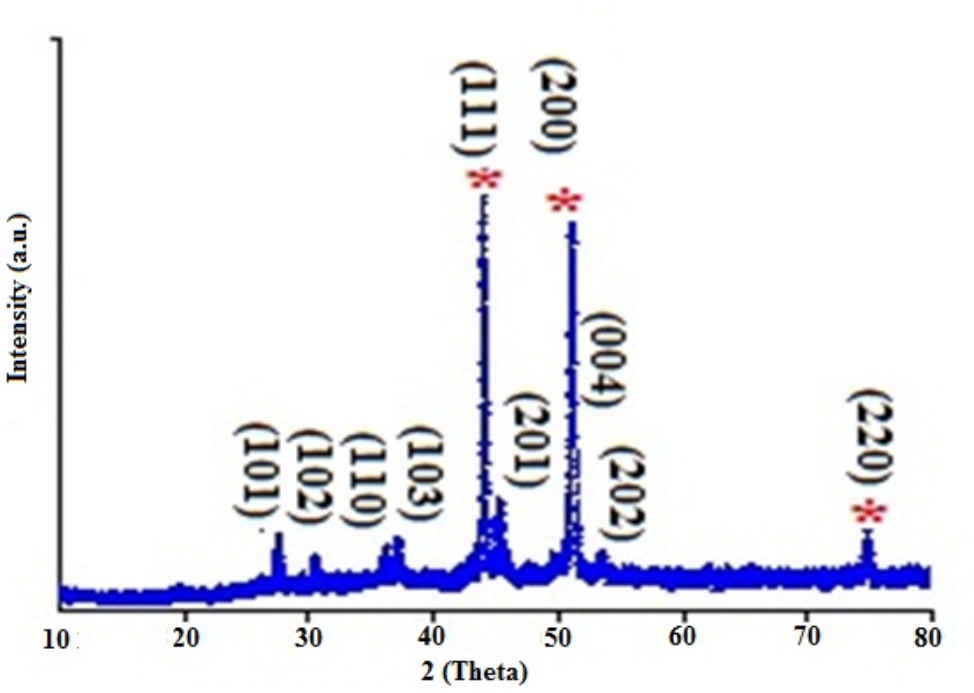

Figure 1.17: X-ray diffraction pattern of a Cu-CdSe-Cu nanowire heterojunctions embedded in AAO template.

The diffraction peaks positioned at values 2**θ** values of 27.62^{o}, 30.56^{o}, 36.16^{o}, 37.18^{o}, 45.35^{o}, 51.30^{o}, 53.56^{o} corresponds to the (101), (102), (110), (103), (201), (004), (202) planes matches well with wurzite structured CdSe with hexagonal phase compared with

JCPDS (File no. 77-2307). The three peaks at 44.04^{o}, 51.06^{o} and 74.80^{o} correspond to (111), (200), (220) planes matches well with face centered cubic (fcc) structured Cu compared with JCPDS (File no. 83-1326). The minor peaks attributed to impurtiy, which is possibly a byproduct of the silver plating step, are also seen in the pattern.

2 (Theta) Degree	d value (Å)	Relative Intensity	Assignment	(hkl)
27.6194	3.22976	2.66	CdSe	(101)
30.5559	2.92574	1.25	CdSe	(102)
36.1553	2.48444	1.45	CdSe	(110)
37.1778	2.41843	2.47	CdSe	(103)
44.0411	2.05616	22.02	Cu	(111)
45.3475	1.99992	4.10	CdSe	(201)
51.0595	1.78732	62.47	Cu	(200)
51.2997	1.78394	45.92	CdSe	(004)
53.5577	1.70969	0.76	CdSe	(202)
74.7951	1.26831	1.85	Cu	(220)

Table 4: XRD peak assignment for a Cu-CdSe-Cu nanowire heterojunctions.

The crystallite size, D, of the nanowires heterojunctions was found from the peak width with the Scherrer's formula [46]:

$$\mathbf{D= 0.94\lambda/B\cos\theta} \qquad (4.1)$$

Where D is the average crystallite size, λ is the x-ray wavelength, B is the full width of height maximum (FWHM) of a diffraction peak, **θ** is the diffraction angle. The crystallite size of the Cu-CdSe-Cu nanowires heterojunctions calculated from Scherer's formula is 47 nm.

4.2 Scanning electron microscopy analysis

The morphological studies of the Cu-CdSe-Cu nanowires heterojunctions were performed after removing these nanowires heterojunctions from the matrix after dissolving the template in 0.5 M NaOH solution at 27°C for 2 hour followed by washing several times with deionised water, then with ethanol, and subsequently drying these in hot air oven at ambient temperature for overnight. The cleaned and dried sample was mounted using a double adhesive carbon tape on a specially designed aluminium stub coated with a layer of gold-palladium alloy using (JEOL, FINE SPUTTER JFC-1100) sputter coating unit and viewed under Scanning Electron Microscope (JEOL, JSM-6510LV) at 20 kV accelerating voltage..

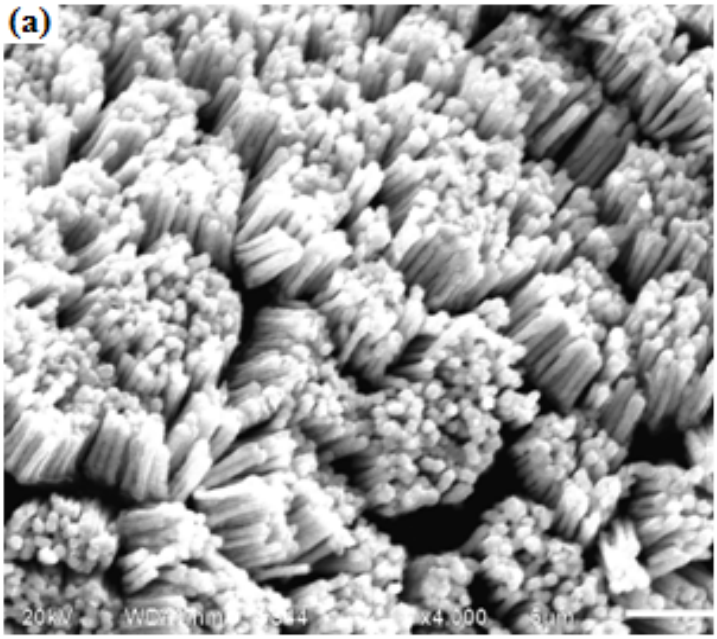

Figure 1.18: The SEM micrographs of bunch Cu-CdSe-Cu nanowires heterojunctions of diameter 300 nm after removal of AAO template

The figures 1.18 and 1.19 show the SEM micrographs of the Cu-CdSe-Cu nanowires heterojunctions at different magnifications. The bunches of Cu-CdSe-Cu nanowires heterojunctions of diameter around 290-300 nm and length 10-15 μm are clearly

observed from the micrographs .The figures 1.19 (b) and 1.19(c) show SEM micrographs at higher magnifications, the arrows in these images indicate the formation of Cu, CdSe, Cu nanowire heterojunctions. It is clear that all the Cu-CdSe-Cu nanowires heterojunctions are not randomly oriented and the length, the diameter, and the growth

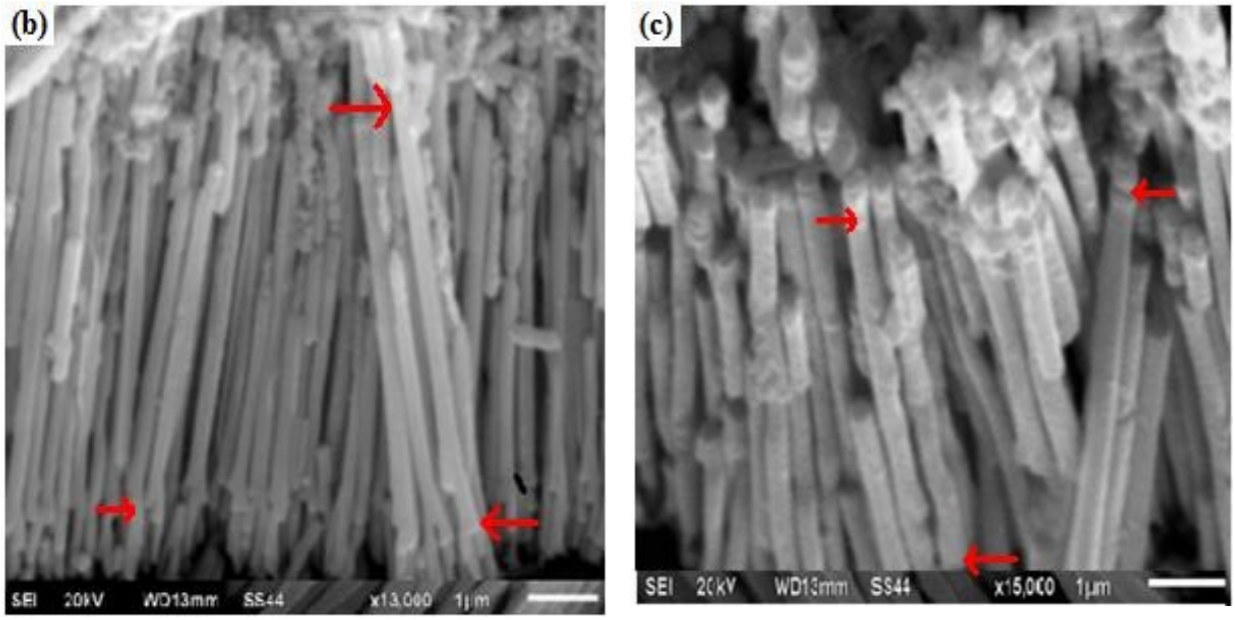

Figure 1.19: Cu-CdSe-Cu nanowires heterojunctions of diameter 300 nm at higher magnification, arrows indicate the Cu, CdSe and Cu heterojunctions

direction of Cu-CdSe-Cu nanowires is quite uniform. The confined growth of nanowires, within the pores of the AAO template leads to the formation of quite uniform and ordered high quality nanowires heterojunctions. These results indicate that the nanowires heterojunctions can be filled uniformly within the pores of the template by electrodeposition.

4.3 Energy dispersive x-ray spectroscopy analysis

For quantitative elemental composition analysis, energy dispersive x-ray spectroscopy (EDAX) of the grown nanowires heterojunctions was carried out by NORAN System SIX

Model 300 attached with the Scanning Electron Microscope (SEM). The chemical composition of the Cu-CdSe-Cu nanowire heterojunctions was determined using energy-dispersive x-ray spectroscopy (EDAX). Electron beam induced inner-shell ionization and subsequent emission of characteristic fluorescence are analyzed in order to obtain the composition. The EDAX spectrum is shown in figure 2(a). The table 1 clearly reveals that nanowires are composed of Cd, Se and Cu, elements and the quantitative analysis indicates their atomic % respectively as 52.88 %, 38.85% and 8.27%. The atomic ratio of Cd and Se has been found to be very close to 1:1 according to stoichiometry. The inset in figure 4.3 shows the selected area for analysis

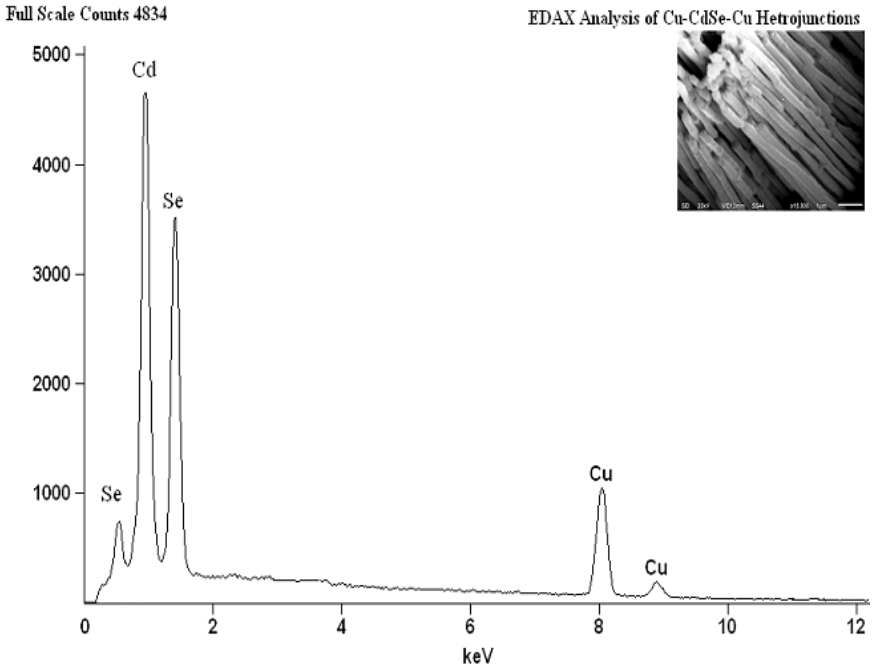

Figure1.20: EDAX spectrum of Cu-CdSe-Cu nanowires heterojunctions; inset shows the area selected for analysis.

Elements	Z	S	Weight %	Atomic %
Cu	29	K-series	8.27	4.01
Cd	48	K-series	52.88	45.32
Se	34	L-series	38.85	50.67

Table 5: EDAX results of sample showing elements, atomic number (Z), series (S), weight %, atomic % of elements present.

4.4 Electrical transport properties

The KEITHLEY source meter, 4200-SCS, attached with ZYVEX S100 Nanomanipulator, with probe size 500 nm, made up of tungsten, was used for collective I–V measurements**.** The figure **1.21** (a) shows the schematic of collective I-V characteristics measurement set up.

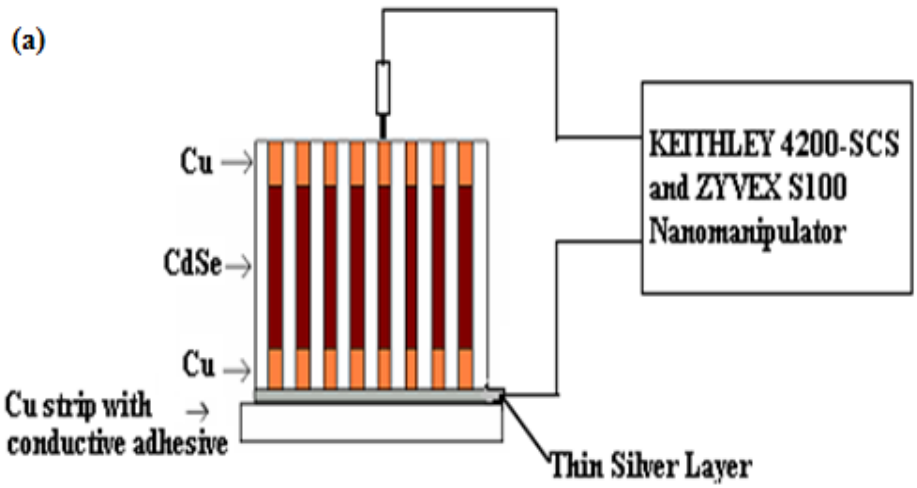

Figure 1.21 (a): The schematic of collective I-V characteristics measurement set up. Generally, when a metal and a semiconductor are brought together, there occurs an energy barrier to electron transportation from the metal side to the semiconductor side at

the metal/semiconductor interface, due to the difference in work functions of the metal and the semiconductor. These nanowire heterojunctions exhibit asymmetric and rectifying behaviour. The observed nonlinearity is caused by the Schottky barriers formed between the nanowires and the metal electrodes at the metal/semiconductor interface. Depending on the height of the Schottky barriers, four distinct I–V characteristics can be observed in nanowire heterojunctions almost linear, symmetric, asymmetric and rectifying [29]. The analysis of the observed I-V characteristics of heterostructures has been carried out making the use of a model based on the single-band effective mass equation [30]. This demands the effective mass of the carriers to be same as that of the bulk material and, with this model, only room temperature I–V characteristics can be analyzed. The figure 1.22 (a) depicts typical I-V curves for 300nm diameter nanowire heterojunctions. The heterostructures of diameter 300nm show rectifying. The Cu-CdSe-Cu heterostructure can be understood as a resistor (CdSe nanowire) sandwiched between two back-to-back Schottky barriers. This resistor is called series resistor ensuing from the undepleted part of the CdSe nanowires. When a positive forward voltage is applied on the metal electrode, Schottky barrier is reverse-biaed on one side and forward-biaed on other side. When a large voltage is applied, the current flowing through the nanowire heterojunctions is sufficiently large and, therefore the applied bias increment is mainly distributed on the nanowires and the corresponding *I–V* curve approaches a straight line with a slope equal to the resistance of the nanowires heterojunctions. The resistance of nanowire heterojunctions was determined using the differential voltage method at large bias I-V curve as [30]

$$\boldsymbol{R = dV_{NW}/dI = a_{NW}dV/dI} \qquad \textbf{(4.4.1)}$$

where $\boldsymbol{R}$ is resistance, $\boldsymbol{dV/dI}$ differential voltage, and $\boldsymbol{a_{NW}}$ voltage drop factor. This

procedure gives resistance 43.43 MΩ for 300 nm diameter nanowire heterojunctions. The intermediate part of I-V curves can be explained using:

$$\ln I = \ln(AJ) = \ln(A) + V(q/kT - 1/Eo) + \ln Js \qquad (4.4.2)$$

where A is the contact area of Schottky barrier, J is the current density through this barrier, E_o is parameter that depends on the density of majority carriers and Js is a slowly varying parameter which depends on the applied voltage [30]. At intermediate bias I-V characteristics were dominated by the reverse-biased Schottky barrier

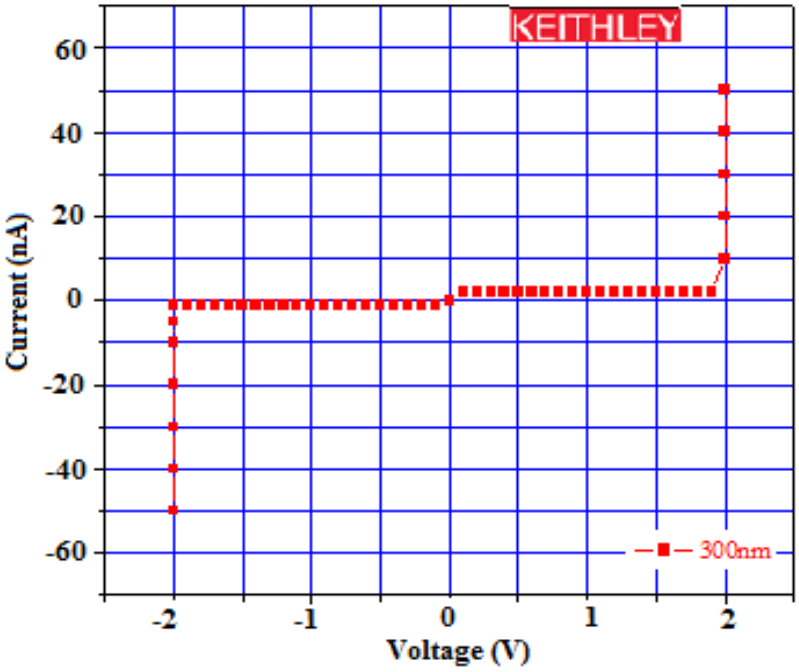

Figure 1.22: Collective two terminal I–V characteristics of Cu-CdSe-Cu nanowire heterojunctions of diameter 300 nm at room temperature.

CHAPTER 5

Conclusion and Future Scope

The aim of this work is the fabrication and characterization of Cu-CdSe-Cu nanowire heterojunctions, by template - assisted technique.

The work has been concluded as follows:

- Highly ordered and uniform Cu–CdSe-Cu nanowires heterojunctions were fabricated by template -assisted electrochemical deposition technique. The growth conditions like pH of solution, temperature of solution, the distance between electrodes etc. has been optimized.

- SEM micrographs graphs reveal the growth and morphology of the Cu-CdSe-Cu nanowires heterojunctions. The bunches of Cu-CdSe-Cu nanowires heterojunctions of diameter around 290-300 nm and length 10-15 μm are clearly observed from the micrographs.

- The XRD pattern reveals that wurzite structured CdSe with hexagonal phase and face centered cubic (fcc) structured Cu has been prepared. The polycrystalline nanowires heterojunctions were fabricated. The crystallite size of the Cu-CdSe-Cu nanowires heterojunctions is found to be 47 nm.

- The composition of the nanowire heterojunctions is characterized by EDAX. The atomic ratio of Cd and Se has been found to be very close to 1:1 according to stoichiometry.

- The length and stoichiometric composition of these nanowires heterojunctions can be well controlled by optimum growth conditions.

The electrodeposition provides a route to fabrication of free-standing metal-semiconductor-metal nanowires. The Electrodeposition of Cu-CdSe-Cu gives polycrystalline nanowire segments, which may be of interest in optical sensing and related applications. These nanowires heterojunctions are more likely to have useful electronic and photovoltaic properties.

REFERENCES:

[1] "Nanotechnology Basics: For students and other learners", center for responsible Nanotechnology, world care 2008

[2] www.nanotechnology.com/docs/wtd015798.pdf

[3] www.nanoscience.com/education/overview.html

[4] Small Wonders, Endless Frontiers: A Review of the National Nanotechnology Initiative, National Research Council, Washington D.C 2002

[5] Nanoscience and Nanotechnologies; Opportunities and Uncertainities, Royal Society and the Royal Academy Of Engineering UK, 2004.

[6] The National Nanotechnology Initiative Strategic Plan, National Science and Technology Council, Washington D.C., December 2002

[7] www.ringsurf.com/online/2003-structures.html

[8] www.nanofm.com/terms/quantum_confinement.html

[9] C.R Martin, Chem. Mater. 8 1739 1996

[10] A Huczko, Appl. Phys. A 70, 365 2000

[11] A D M Lai, R.B Jason, Journal of Colloid and Interface Science 323 203 2008

[12] G Cao, D Liu, Advances in Colloid and Interface Science 136 45 2008

[13] Y Li, F Qian, J Xiang, C M Lieber, Mateials today 9 10 2006

[14] Haydena, Oliver, R Agarwal, W Luc. Nano today 3 5 2008

[15] E Maria, M Toimil, B Veronique, D Dobri, N Reinhard, S Roland, S U Ingrid, J Vetter, Adv. Mater 13 2001

[16] S Kumar, S K Chakarvarti, Current Science 5 87 2004

[17] S Kumar, S K Chakarvarti, Digest Journal of Nanomaterials and Biostructures 1 139 2006

[18]G Tao, G Meng, Y Wang, S Sun, L Zhang J. Phys.Condense Matter 14 355 2002

[19] R Kaur, N K Verma, S K Chakarvarti, J Mater. Sci 42 3588 2007

[20] R Kaur, N K Verma, S K Chakarvarti, J Mater. Sci 42 8083 2007

[21] S Kumar, Kumar Sanjeev, N K Verma, S K Chakarvarti, J K Sharma, Digest Journal of Nanomaterials and Biostructures 3 199 2008

[22] D Xu, D Chen, Y Xu, X Shi, G Guo, L Guim, Y Tang, Pure Appl. Chem., 72 127 2000.

[23] U A Jeong, Y Xia, A Yadong, B Yin Chemical Physics Letters 416 246 2005

[24] L Xi, B Chris, M L Yeng Chem. Mater. 21 1465 2009

[25] S P Mondal, K Das, A Dhar, S K Ray, IEEE 978 1478 2007.

[26] S Patole, M Islam, R C Aiyer, M Shailaja, J Mater Sci 41 5602 2006

[27] R Singh, R Kumar, S K Chakarvarti, Physica E 40 591 2008

[28] M Chaudhri, A Vohra, S K Chakarvarti, Materials Science and Engineering B

[29] Z Zhang, K Yao, Y Liu, C Jin, X Liang, Q Chen, L M Peng, Adv. Funct. Mater. 17 2478 2008

[30] A Bose, K Chatterjee, D Chakravorty, Bull. Materials Science 32 227 2009

[31] D J Pen, J K N Mbindyo, A J Carado, E M Thomas, D K Christine, R Baharak, M S Theresa S. J. Phys. Chem 106 458 2002

[32] M. S. Dresselhausa, Y.M. Linb, O. Rabinc, M.R. Blackb, G. Dresselhausd.

[33] M A Lai, D R Jason , Journal of Colloid and Interface Science 323 203 2008

[34] R C Furneaux, W.R. Rigby, and A P Davidson, Nature 337 147 (1989).

[35] R L Fleisher, P B Price, and R M Walker, Nuclear Tracks in Solids, University of California Press Berkeley CA 1975.

[36] R J Tonucci, B L Justus, A J Campillo, and C E Ford, Science 258 783 (1992).

[37] G E Possin, Rev. Sci. Instrum. 41 772 (1970).

[38] C Wu and T. Bein, Science 264 1757 (1994).

[39] S Fan, M G Chapline, N R Franklin, W Tombler, A M Cassell, H Dai, Science 283 5 12 1999

[40] P Enzel, J J Zoller, and T Bein, Chem. Commun. 633 1992.

[41] C Guerret-Piecourt, Y Le Bouar, A Loiseau, and H Pascard, Nature 372 761 1994.

[42] P M Ajayan, O Stephan, P Redlich, and C Colliex, Nature 375 564 1995

[43] J B Mohler, H J Sedusky, Electroplating for the Metallurgist, Engineer and Chemist. New York: Chemical Publishing 57 129 1951.

[44] F R N Nabarro, P J Jackson, R H Doremus, B W Roberts, D Turnbull, editors. Growth and Perfection of Crystals. New York JohnWiley, 2 edition 1958.

[45] T M Whitney, J S Jiang, P C Searson, C L Chien, Science 261 1316 1993

[46] B D Cullity and S R Stock, Element of X-Ray Diffraction, 3rd Edition, Prentice hall, upper saddle river NJ 4th edition 2001.

[47] E F Kaeble, Handbook of X-Rays, Mcgraw-Hill, New York, 4th edition 1967.

[48] M C Veronica, C R Martin, J. Phys. Chem. B, 102 9985 1998

[49] Nanotechnology Measurement Handbook A Guide to Electrical Measurements for Nanoscience Applications 1st Edition, KEITHLEY.

[50] J.S Preston, The Constitution and Mechanism of the Se Rectifier Photo, Proc. Roy.Soc. (Lond.) Series A 202 449

[51] Pallab Bhattacharya, Semiconductor Optoelectronic Devices, Prentice Hall, 1997

[52] J Tersoff, Physical Review B, 30, 4874, 1984

[53] N Debbar et al., Physical Review, B40, 1058, 1989

[54] Sergei A. Ivanov, Andrei Piryatinski, Jagjit Nanda, Sergei Tretiak, Kevin R. Zavadil, William O. Wallace, Don Werder and Victor I. Klimov, J. Am. Chem. Soc. 129 11708 2007

[55] Istvan Robel, Masaru Kuno and Prashant V Kamat, J. Am. Chem. Soc.129 4136 2007

[56] H Kroemer, Proceedings of the IEEE, Vol. 51, pp. 1782–1783, 1963

[57] Virginia Semiconductor, The General Properties of Si, Ge, SiGe, SiO2 and Si3N4, Springer Pub. 4th edition 2002

[58] Min Lai a, D Jason, Riley b, Journal of Colloid and Interface Science 323 203–212 2008